A theoretical analysis of the resolution due to diffusion and size dispersion of particles in deterministic lateral displacement devices

Martin Heller and Henrik Bruus

Department of Micro- and Nanotechnology, Technical University of Denmark,
DTU Nanotech, Building 345 East, DK-2800 Kongens Lyngby, Denmark

E-mail: Martin.Heller@nanotech.dtu.dk and Henrik.Bruus@nanotech.dtu.dk

Abstract
We present a model including diffusion and particle-size dispersion for the separation of
particles in deterministic lateral displacement devices also known as bumper arrays. We
determine the upper critical diameter for diffusion-dominated motion and the lower critical
diameter for pure convection-induced displacement. Application of our model to data suggests
that the systematic deviation, observed for small particles in several experiments, from the
critical diameter for separation given by simple laminar flow considerations may be explained
by diffusion and size dispersion.

1. Introduction

In 2004, Huang *et al* [1] developed the elegant method of
particle separation by deterministic lateral displacement in so-
called microfluidic bumper arrays. The method, which relies
on the laminar flow properties characteristic of microfluidcs,
shows a great potential for fast and accurate separation of
particles on the micrometer scale [1–4]. Among the key
assets of the deterministic lateral displacement separation
principle are that clogging can be avoided because particles
much smaller than the feature size of the devices can be
separated, that the devices are passive, i.e. the particles bump
into solid obstacles or bumpers, and that the separation process
is continuous.

More precisely, particle transport in microfluidic bumper
arrays is primarily governed by convection due to the fluid
flow and by displacement due to interaction with the bumpers
in the array [1]. These processes are deterministic and the
critical diameter for separation of relatively large particles in
these devices is well understood in terms of the width of flow
lanes bifurcating around the bumpers in the periodic arrays
[3]. However, if bumper arrays and particles are scaled down,
diffusion will influence the separation process and affect the
critical particle size significantly. Previously reported data

on separation of particles in bumper arrays all show a bias
toward larger critical particle size than that given by the width
of the flow lanes nearest to the bumpers of the array [1–3]. In
this work we extend existing models by adding diffusion and
taking particle-diameter dispersion into account, and thereby
explain the observed discrepancy.

In bumper arrays particles are convected by the fluid flow
through an array of bumpers placed in columns separated by
the distance λ in the flow direction, see figure 1(*a*). For a given
integer N, the array is made N-periodic in the flow direction
by displacing the bumpers in a given column a distance λ/N
perpendicular to the flow direction with respect to the bumper
positions in the previous column. Due to this periodicity of the
array and the laminarity of the flow, the stream can naturally
be divided into N lanes, each carrying the same amount of
fluid flux, and each having a specific path through the device,
see [1].

For a given steady pressure drop, the fluid in the device
moves with an average velocity u_0. Assuming a parabolic
velocity profile $u(x)$ in the gap of width w_g between two
neighboring bumpers, see figure 1(*b*),

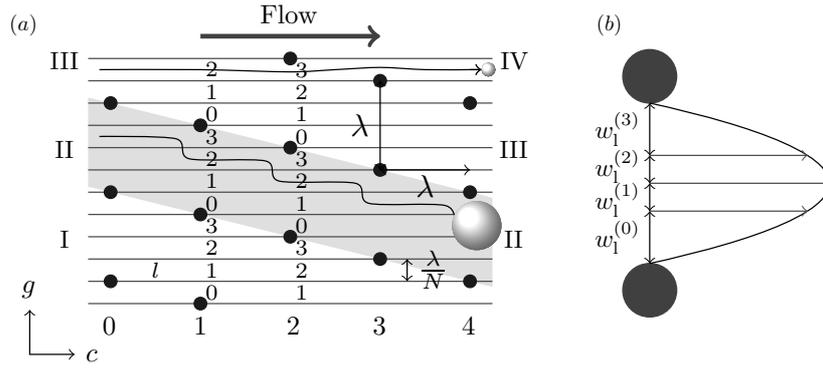$$u(x) = 6u_0 \frac{x}{w_g} \left(1 - \frac{x}{w_g} \right), \tag{1}$$

Figure 1. (*a*) An array of bumpers (black dots) with the definition of the lane number *l* (small arabic numbers), the column number *c* (large arabic numbers) and the gap number *g* (roman numbers). The shaded region illustrates how the shift in the position of gap II follows the geometry of the array. Large particles following the displacement path will therefore stay in the same gap number and lane number throughout the entire array as illustrated by the skew bumping trajectory of a large particle (large illuminated sphere). Small particles will not be displaced by the bumpers and will therefore visit all lane numbers as they follow the so-called zigzag path through an entire period of the array [1]. This is illustrated by the almost horizontal trajectory of a small particle in the upper flow lane (small illuminated sphere). (*b*) Close-up of a single gap between two bumpers (disks) in the array. Each of the four flow lanes carries the same flow rate. Due to the parabolic flow profile in the gap region, the width $w_1^{(l)}$ of the flow-lane *l* depends on its position in the gap.

the total flow rate Q_{tot} is given by

$$Q_{\text{tot}} = \int_0^{w_g} u(x)\, \mathrm{d}x = w_g u_0. \tag{2}$$

By numerical simulations at low Reynolds numbers relevant for the actual devices, $Re \approx 10^{-3} - 10^{-2}$, we find the assumption of a parabolic flow profile in the gap region well justified. This also agrees with the usual estimate for the entrance length $l_{\text{entr}} = 0.06 Re\, w$, which is here of the order of 1 nm.

For an *N*-periodic array, the *N* flow lanes in a given gap carry the same flow rate Q_{tot}/N. The width $w_1^{(l)}$ of lane *l* is found by solving

$$\frac{Q_{\text{tot}}}{N} = \int_{x^{(l)}}^{x^{(l)}+w_1^{(l)}} u(x)\, \mathrm{d}x, \tag{3}$$

where $x^{(l)} = \sum_{j=0}^{l} w_1^{(j)}$ is the starting position of lane *l*. In the simple bifurcating flow-lane model [1, 3] the critical diameter d_c is given as $d_c/2 = w_1^{(1)}$. A small particle with $d < d_c$ will never leave its initial flow lane and will thus be convected in the general flow direction following a so-called zigzag path. The conventionally used name zigzag path refers to the case where the bumpers are large compared to their center-to-center distance. In this case the path, which appears almost straight in figure 1 given the smallness of the bumpers, becomes truly zigzag-shaped [1]. Large particles with $d > d_c$ will quickly bump against a bumper and from then on be forced by consecutive bumping to follow the skew direction of the array geometry, the so-called displacement path. When a particle gets bumped by a bumper in the array it will be displaced perpendicular to the flow direction until its center is located one particle radius $d/2$ from the surface of the bumper. This corresponds to n_1 lanes of displacement,

$$n_1 = \frac{N}{w_g u_0} \int_0^{d/2} u(x)\, \mathrm{d}x = N \frac{d^2}{4w_g^2}\left(3 - \frac{d}{w}\right). \tag{4}$$

In the bulk fluid, where the lanes are assumed to have equal width λ/N, see figure 1(*a*), the displaced distance ℓ_{disp} is therefore

$$\ell_{\text{disp}}(d) = n_1 \frac{\lambda}{N} = \lambda \frac{d^2}{4w_g^2}\left(3 - \frac{d}{w_g}\right). \tag{5}$$

In this work we extend the simple bifurcating flow-lane model by including diffusion and particle-diameter dispersion.

2. Model including diffusion

During the average time $\tau = \lambda/u_0$ it takes a particle to move by convection from one column to the next, it also diffuses. We assume that the diffusion process perpendicular to the flow direction is normally distributed with mean value zero and variance

$$\sigma^2 = 2D\tau, \tag{6}$$

where the diffusivity D is given by the Stokes–Einstein expression

$$D = \frac{k_B T}{3\pi \eta d}. \tag{7}$$

Here k_B is Boltzmann's constant, T is the temperature and η is the viscosity of the fluid. Throughout the paper we use this expression to calculate D for any given particle size.

In figure 2 are sketched the two limits of (*a*) a small strongly diffusing particle, for which the interaction with the bumpers as well as the role of the flow lanes is negligible, and (*b*) a large particle, for which diffusion rarely brings the particle out of its given lane, and where each bumping event resets the position of the particle.

Note that we do not model Taylor–Aris dispersion explicitly. The reason is that this convection–diffusion phenomenon mainly affects the particle distribution along the flow direction [5]. However, we are not interested in the detailed arrival times of the particles in the outlet, only in their transverse distribution.
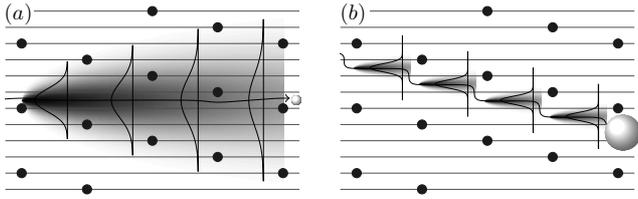
Figure 2. (*a*) The motion of very small particles is dominated by diffusion. Their distribution at the end of the array is therefore determined by their transverse diffusion during the time spent in the array. The intensity of the shaded region indicates the probability for finding the small particle at a given position in the array. A non-diffusive particle would follow the solid black trajectory straight through the array. (*b*) Large particles diffuse as well—but not very much—and every time they interact with a bumper their position in the gap is reset to the particle radius. Large particles therefore only have a slight probability of escaping the displacement path represented by the full black line. In both panels the Gaussian distribution of the diffusing particles is shown at four cross-sections.

2.1. Diffusion model

In order to escape bumping, a particle must diffuse more in the time interval τ than the difference $\ell_{disp} - \lambda/N$ between the bulk displacement and the shift in position of the next bumper. The probability p_{esc} for this to happen is given by the integral of the Gaussian tails (see figure 2) in the neighboring lanes, i.e., by the error function

$$p_{esc}(d) = \frac{1}{2} - \frac{1}{2}\,\text{erf}\left(\frac{\ell_{disp}(d) - \frac{1}{N}\lambda}{\sqrt{2}\sigma(d)}\right), \qquad (8)$$

where we have introduced the d-dependence explicitly. When a particle is transported through a bumper array it must bump at every bumper within one period of the array in order to be displaced one gap at the outlet. Thus, if the particle escapes at least one time in N attempts, it will not be displaced. We define the critical particle size d_c to be the size for which half of the particles escape bumping as they pass one period of the array. Thus d_c can be found by solving

$$\sum_{k=1}^{N}\binom{N}{k}p_{esc}(d_c)^k[1 - p_{esc}(d_c)]^{N-k} = \frac{1}{2}. \qquad (9)$$

In figure 3 we have plotted the result of our model calculation for the critical particle sizes as a function of the bumper period for parameter values corresponding to the bumper arrays used by Inglis *et al* [3] (full line), Huang *et al* [1] (dashed line) and Larsen [6] (dotted line). The corresponding measured data points from these papers are plotted as circular, square and triangular points, respectively.

It must be emphasized that although the authors of [3] in their text only describe bumper arrays with a relative column displacement $\varepsilon = 1/N$, they do plot, without comments, data points with other displacements, e.g., $\epsilon = 0.3$. These non-$1/N$ bumper arrays lead to more complicated displacement characteristics. This interesting topic, which we are currently studying, goes beyond the scope of the present work, where we focus on the influence of diffusion and particle-size distribution on the more simple and most widely used $1/N$-bumper arrays. In figure 3, we have therefore only plotted data points from [3] with $\epsilon = 1/N$.
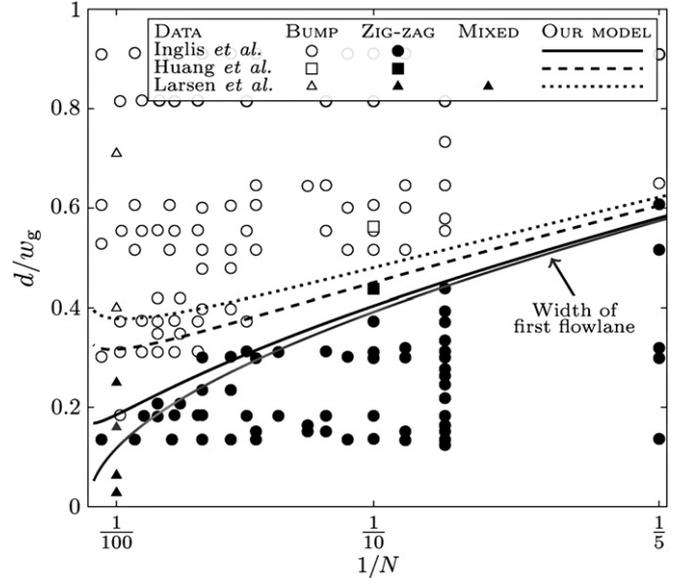

Figure 3. Our model applied to the experimental data of Inglis *et al* [3], Huang *et al* [1] and Larsen [6]. Particle diameter d over the gap width w_g is plotted as a function of the inverse period $1/N$. The full, dashed and dotted black lines show the theoretically predicted critical particle size for the bumper arrays used by Inglis *et al* [3] (only points with $\varepsilon = 1/N$), Huang *et al* [1] (only for $N = 10$) and Larsen [6] (only for $N = 100$), respectively. The experimental data points are representing particles following bumper paths (open symbols), zigzag paths (solid black symbols) and neither of these paths (solid gray symbols).

2.2. Comparison with experiments

The observation that the critical particle size in a $1/N$ bumper device is larger than the width of the first flow lane is also supported by the experimental data in figure 2 of [3]. Our model suggests that the deviation of the critical particle size from the width of the first flow lane can be explained by diffusion of the particles. In figure 3 it is seen how well the theoretical lines predict the transition between zigzag paths and displacement paths: the full line divides open and closed circles, the dashed line divides open and closed squares, and the dotted line divides open and closed triangles.

Using parameter values corresponding to the bumper device presented by Huang *et al* [1] our model predicts a critical particle diameter of 0.45 times the width of the gap for the particles traveling through the device with an average velocity of $400\,\mu\text{m s}^{-1}$. This is in good agreement with figure 2(*a*) in [1].

3. A discrete model including diffusion and dispersion

Particles typically used in experiments on particle separation are not mono-disperse. Their average diameters are distributed around a certain mean value with a relative standard deviation $\Delta d/d$, which typically is 20%, 10% and 5% for particles with $d = 25$ nm, $d = 100$ nm and $d = 500$ nm, respectively.

Faced with such a size dispersion it is very useful to have a simple method for predicting its effect. In the following
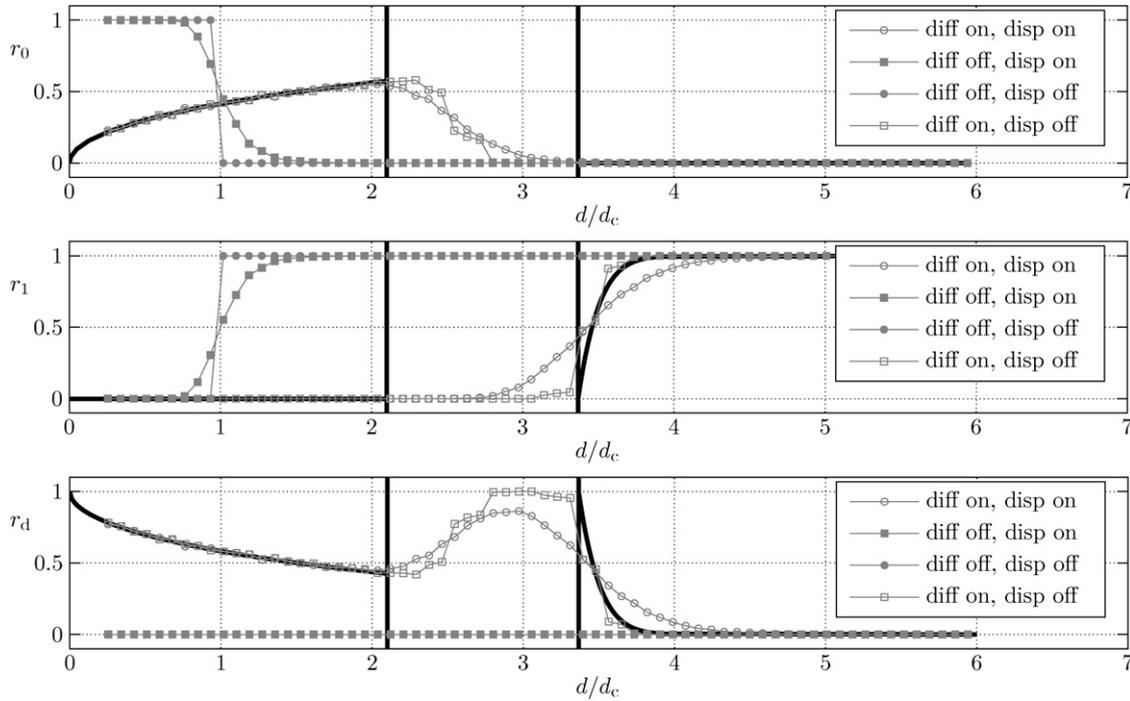
Figure 4. Relative numbers r_0, r_1 and r_d of particles following the zigzag path, the displacement path and neither of these two paths, respectively, plotted as a function of the normalized, average particle diameter d/d_c, where $d_c = 118$ nm. The parameters of the bumper array are taken from [6]: $N = 100$, $\lambda = 8$ μm, $w_g = 1$ μm, $L = 20N\lambda = 16$ mm and $u_0 = 250$ μm s^{-1}. The buffer liquid is water at room temperature. Neglecting diffusion (solid symbols), the particles follow the zigzag path if $d < d_c$ and the displacement path if $d > d_c$. Including diffusion (open symbols), with D given by equation (7), the small particles are not influenced by the bumpers. For $d > 2.1d_c$ the influence of the bumpers sets in, and for $d > 3.4d_c$ the particles follow the displacement path. The full black curves are the predictions using the results in sections 3.4.1 and 3.4.2, while the thick black vertical lines indicate the particle size when small particles stop behaving purely diffusive (left-most lines) and when large particles begin a purely deterministic displacement (right-most lines).

we therefore introduce a discrete model of the transport of particles with different diameters d in an N-periodic bumper array taking convection, diffusion and size dispersion into account. The model allows us to study the relative influence of all three phenomena on the separation efficiency in a fast and simple manner. We illustrate our model by using the specific parameters from the bumper device presented in [6], see figure 4. In particular our results suggest that the critical size for separation or displacement, studied above, must be supplemented by a smaller critical size below which pure diffusion governs the motion of the particles in the bumper array. This prediction has not yet been tested experimentally.

3.1. Definition of the discrete model

At any instant, a particle is assumed to be positioned in the center of a flow lane l of gap g in some column c of the array. For simplicity we further assume that the size distribution of any given set of particles is a normal distribution with a mean value given by the size quoted by the manufacturer and a relative standard deviation of 10%.

By convection any given particle moves from one column to the next. If it ends up in the last lane ($l = N - 1$) in one gap, it will be shifted to the first lane ($l = 0$) in the subsequent gap. Otherwise it will stay in the current gap and move up one

lane. In our model pure convection is therefore described by the discrete map

$$(c, g, l) \mapsto \begin{cases} (c + 1, g + 1, 0), & \text{if } l = N - 1, \\ (c + 1, g, l + 1), & \text{otherwise.} \end{cases} \quad (10)$$

Because of the finite diameter d of the particle there is a minimum and a maximum lane number that it can occupy. The minimum lane number is the smallest integer $l_{\min}$ that satisfies

$$\sum_{l=0}^{l_{\min}} w_1^{(l)} > \frac{d}{2}. \quad (11a)$$

Similarly, the maximum lane number $l_{\max}$ is the largest integer that satisfies

$$\sum_{l=l_{\max}}^{N-1} w_1^{(l)} > \frac{d}{2}. \quad (11b)$$

Consequently, the simple convection mapping from equation (10) needs to be modified to account for the finite size of the particles

$$(c, g, l) \mapsto \begin{cases} (c + 1, g + 1, l_{\min}), & \text{if } l = N - 1, \\ (c + 1, g, l + 1), & \text{if } l < l_{\max} - 1, \\ (c + 1, g, l_{\max}), & \text{otherwise.} \end{cases} \quad (12)$$

The above convection scheme accounts for the separation of particles in deterministic lateral displacement devices

according to size. The critical particle diameter predicted by this model is

$$d_c = 2w_1^{(0)} \tag{13}$$

in accordance with the geometric arguments of [3].

To characterize the separation quantitatively, we define the relative particle numbers r_0, r_1 and r_d as

$$r_0 = \text{relative number of particles} \\ \text{following the zigzag path}, \tag{14a}$$

$$r_1 = \text{relative number of particles following} \\ \text{the displacement path}, \tag{14b}$$

$$r_d = \text{relative number of all other particles}. \tag{14c}$$

With these definitions the sum $r_0 + r_1 + r_d$ is always unity. If $r_0 = 1$ all particles follow the zigzag path and if $r_1 = 1$ all particles follow the displacement path. If $r_d \neq$ some of the particles end up at positions not explained by the deterministic analysis of the separation process. In figure 4 we have plotted the relative particle numbers r_0, r_1 and r_d as a function of the average particle diameter d.

3.2. Pure mono-disperse convection

For mono-disperse and non-diffusing particles, the model results, as expected, in two modes: the zigzag mode and the displacement mode, see the closed circles in figure 4. For $d < d_c$ we have $r_0 = 1$, and for $d \geqslant d_c$ we have $r_1 = 1$, while we always have $r_d = 0$. The relative particle numbers can therefore be written as

$$(r_0, r_d, r_1) = \begin{cases} (1, 0, 0) & \text{for} \quad d < d_c, \\ (0, 0, 1) & \text{for} \quad d \geqslant d_c. \end{cases} \tag{15}$$

3.3. Influence of size dispersion

If we assume that the particles are not mono-disperse, but are distributed around a mean size d with standard deviation Δd, the shift as a function of d from the zigzag mode to the displacement mode happens gradually instead of abruptly at a certain critical size d_c (figure 4, closed squares). The relative number of particles following the zigzag path r_0 can be found by integrating over all particle sizes smaller than the critical diameter given by the array geometry

$$r_0 = \int_{-\infty}^{d_c} \frac{1}{\sqrt{2\pi(\Delta d)^2}} \exp\left(\frac{-(s-d)^2}{2(\Delta d)^2}\right) ds. \tag{16a}$$

Similarly, the relative number of particles following the displacement path r_1 can be found by integrating over all particle sizes larger than d_c

$$r_1 = \int_{d_c}^{\infty} \frac{1}{\sqrt{2\pi(\Delta d)^2}} \exp\left(\frac{-(s-d)^2}{2(\Delta d)^2}\right) ds. \tag{16b}$$

The system is still a bi-modal system because $r_d = 0$ for all particle sizes.

3.4. Influence of diffusion

In 1D during the time step τ a particle diffuses the distance ℓ, the average of which is the size-dependent diffusion length $\sigma(d)$ given by

$$\sigma(d) = \langle \ell \rangle = \sqrt{2D\tau} = \sqrt{2\frac{k_B T}{3\pi \eta d} \frac{\lambda}{u_0}}. \tag{17}$$

In our model we discretize the transverse diffusion as the properly rounded number n_{jump} of flow lanes crossed by the particle during diffusion,

$$n_{jump} = \frac{N}{\lambda} \ell. \tag{18}$$

The addition of diffusion smears out the displacement of the particles and causes the critical diameter to be larger than in the diffusion-less case (figure 4, open symbols).

3.4.1. Bumping criterion for small particles.
Very small particles are completely dominated by diffusion, and the particle distribution at the end of the array is simply given by the transverse diffusion of the particles during the time L/u_0 it takes for the particle to be convected all the way L through the array, see figure 2(a). For small particles we therefore have

$$r_0 = \int_{-\frac{3}{2}\frac{\lambda}{N}}^{\frac{3}{2}\frac{\lambda}{N}} \frac{1}{\sqrt{2\pi\sigma^2}} \exp\left(\frac{-x^2}{2\sigma^2}\right) dx, \tag{19}$$

where $\sigma^2 = 2DL/u_0$. In figure 4 we have plotted r_0 versus d/d_c and $r_d = 1 - r_0$ as the thick black curves in the interval $0 < d/d_c < 2.1$.

As the particle diameter d is increased, the bumpers begin to become important as the diffusion length $\sigma(d)$, equation (17), is decreased and becomes equal to the displacement length ℓ_{disp}, equation (5). Using the criterion $\sigma(d_1) = \ell_{disp}$, with the parameter values used in figure 4, we find that particles stop behaving as small diffusion-dominated particles and start interacting with the bumpers when $d_1 = 2.1d_c$. This cross-over value is indicated by the left-most vertical lines in figure 4, and it fits well with the simulation data. Note that the specific value of the pre-factor is determined for $d_c = 118$ nm.

3.4.2. Bumping criterion for large particles.
Large particles will interact with the bumpers at every row in the array and their position is thus reset at every bump to be ℓ_{disp}, see figure 2(b). Diffusion can therefore be neglected for such particles, they all follow the displacement path, and $r_1 = 1$.

As the particle diameter is lowered, the probability p_{esc} that a particle escapes the displacement path can be estimated by the probability of diffusing from the displaced position to the last flow lane in the gap, i.e. the distance $\ell_{disp} - \frac{\lambda}{N}$. This probability p_{esc} is given by equation (8). In figure 4 we have plotted $r_d = p_{esc}$ and $r_1 = 1 - r_d$ as thick black curves in the interval $3.4 < d/d_c < 6$.

In order to follow the displacement path, a particle must bump at each row in the array. If we consider an N-periodic array with m full periods, the particles will have mN bumping opportunities as they pass through the entire array. If a particle
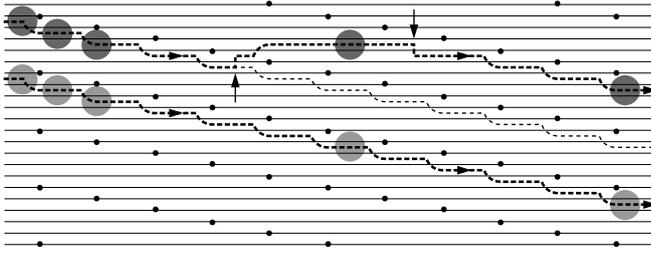
Figure 5. Schematics of a $N = 5$ bumper array (black dots) in which a large particle (light gray) moves along the displacement path (lower thick dashed line) without diffusion, and another particle of the same size (dark gray) moves partially along the displacement path (upper thick dashed line) under the influence of diffusion. The corresponding displacement path without diffusion is also shown (thin dashed line). Two diffusion-induced jumping events, each causing the particle to jump to a neigboring lane, are marked by the vertical arrows. The upward event induces a shift in the gap number by one, while the downward event does not induce a shift in the gap number. The diffusing particle thus exits the bumper array one gap above its diffusionless counter part.

evades bumping at a bumper, it will be convected by the flow through a full period of the array before bumping is possible again. Because of the escape, it will miss N bumping opportunities and end up one gap from the displacement path, see figure 5. Consequently, if a particle escapes one time, it will only have $(m - 1)N$ bumping opportunities and has therefore escaped bumping with a probability of $1/[(m-1)N]$. The upper critical particle size d_2 for convection-induced displacement is defined using equation (8) as

$$p_{\text{esc}}(d_2) = \frac{1}{(m-1)N}. \tag{20}$$

For the device used in the experiments by Larsen [6] we find $d_2 = 3.4d_c$. The predicted upper limit for diffusion dominated motion and the lower limit for convection-induced displacement compares well with the experimental observation by Larsen [6] that some particles end up in a transition region between the displacement path and the zigzag path (figure 3, gray triangles). Based on the data for $1/N = 1/100$ in figure 3 the experimentally observed transition region begins at $d_1 = 0.16w_g = 1.4d_c$ (the highest lying gray triangle) and ends at $d_2 = 0.40w_g = 3.4d_c$ (the lowest lying white triangle). Considering the simplicity of the discrete model this is in fair agreement with our model predictions, $d_1 = 2.1d_c$ and $d_2 = 3.4d_c$.

4. Conclusion

Experimental data on separation of particles in bumper arrays all show a systematic deviation from predictions made from the bifurcating flow-lane model [1, 3, 6]. Application of the model presented in this paper to the available data suggests that this systematic deviation may be explained by diffusion. In addition, we have proposed a simple discrete model for quickly simulating particle separation in bumper arrays. In contrast to the single critical particle size found in earlier analyses based solely on the deterministic separation processes, our work including diffusion identifies two particle sizes characteristic for the separation in bumper arrays: a small particle size d_1 below which diffusion dominates and a larger particle size d_2 above which the deterministic processes govern the sorting. Particles of intermediate sizes will neither follow the average flow direction nor the direction set by the array geometry. If bumper devices are scaled down both d_1 and d_2 are larger than the critical size predicted in the existing literature.

The presented model takes particle diffusion and size dispersion into account and has been validated against experimental data for a bumper device with period $N = 100$. In this example the transition from zigzag paths to displacement paths happens at particle sizes in the interval from 2.1 to 3.4 times the critical particle size predicted from geometrical arguments. This transition interval is in qualitative correspondence with the experimental observations from Larsen [6]. Our discrete model and the estimates presented in this paper suggest that particles smaller than twice the geometrical critical size of the $N = 100$ bumper device behave diffusively and are not affected by the bumpers because the small diffusive particles rarely come into contact with the bumpers due to random Brownian motion. We believe that our discrete model will be useful for design and evaluation of bumper arrays with any given specification.

References

[1] Huang L R, Cox E C, Austin R H and Sturm J C 2004 *Science* **304** 987–90
[2] Zheng S, Yung R, Tai Y-C and Kasdan H 2005 *Proc. 18th IEEE Int. Conf. on Micro Electro Mechanical Systems (Miami, USA)* pp 851–4
[3] Inglis D W, Davis J A, Austin R H and Sturm J C 2006 *Lab Chip* **6** 655–8
[4] Davis J A, Inglis D W, Morton K J, Lawrence D A, Huang L R, Chou S Y, Sturm J C and Austin R H 2006 *Proc. Natl Acad. Sci.* **103** 14779–84
[5] Bruus H 2008 *Theoretical Microfluidics* (Oxford: Oxford University Press)
[6] Larsen A V 2006 Deterministic bio separation devices *MSc Thesis* Technical University of Denmark www.nanotech.dtu.dk/NSE-optofluidics